A UNIQUE FLIGHT TEST FACILITY: DESCRIPTION AND RESULTS

Robert R. Meyer, Jr.

November 1982

NASA

NASA Technical Memorandum 84900

A UNIQUE FLIGHT TEST FACILITY: DESCRIPTION AND RESULTS

Robert R. Meyer, Jr.
Ames Research Center
Dryden Flight Research Facility
Edwards, California

A UNIQUE FLIGHT TEST FACILITY: DESCRIPTION AND RESULTS

Robert R. Meyer, Jr.*
NASA Ames Research Center
Dryden Flight Research Facility
Edwards, California

Abstract

The Dryden Flight Research Facility has developed a unique research facility for conducting aerodynamic and fluid mechanics experiments in flight. A low aspect ratio fin, referred to as the flight test fixture (FTF), is mounted on the underside of the fuselage of an F-104G aircraft. The F-104/FTF facility is described, and the capabilities are discussed. The capabilities include (1) a large Mach number envelope (0.4 to 2.0), including the region through Mach 1.0; (2) the potential ability to test articles larger than those that can be tested in wind tunnels; (3) the large chord Reynolds number envelope (greater than 40 million); and (4) the ability to define small increments in friction drag between two test surfaces. Data are presented from experiments that demonstrate some of the capabilities of the FTF, including the shuttle thermal protection system airload tests, instrument development, and base drag studies. Proposed skin friction experiments and instrument evaluation studies are also discussed.

Nomenclature

C_{D_b} base drag coefficient

C_f local friction coefficient

C_p pressure coefficient, $\dfrac{p - p_\infty}{\bar{q}}$

C_p^* critical or sonic pressure coefficient

c local chord

DFRF   Dryden Flight Research Facility

FTF   flight test fixture

h boundary layer rake probe height, dimension given from surface to center of probe

M Mach number

p local static pressure

p_{t_1} total pressure ahead of shock

p_{t_2} total pressure behind shock

pcm   pulse code modulation

$\bar{q}$ dynamic pressure, $0.7M^2 p$

R Reynolds number

---

*Aerospace Engineer

STS-1   first shuttle flight (space transportation system 1)

T absolute temperature

TPS   thermal protection system

x chordwise distance from leading edge, positive aft

y spanwise distance from root, positive down

u/u_e velocity ratio, local velocity/edge velocity

α angle of attack

β angle of sideslip

Δ increment

δ boundary layer thickness

δ^* boundary layer displacement thickness

μ absolute viscosity

Subscripts:

avg   average condition

e   edge condition

FTF   based on flight test fixture

θ based on momentum thickness

∞ referenced to calculated free-stream conditions

Superscript:

$(\ )'$ based on reference temperature method

Introduction

Experimental aerodynamic and fluid mechanics investigations are primarily conducted in ground-based wind tunnel facilities such as those inventoried in Ref. 1. However, these wind tunnel facilities often impose certain limitations on the experimental investigator, such as scale effects due to unit Reynolds number, size limitations for models or test specimens due to test section dimensions, improper scaling of noise or turbulence levels in the wind tunnel, and unreliable data near a Mach number of 1.0 due to problems such as shocks reflected off the tunnel walls. Another limiting factor in ground facilities is the need to conduct tests in several wind tunnels to span a wide range of Mach numbers (for example, incompressible speeds to about twice the speed of sound, which are representative of present fighter/interceptor aircraft). In some instances, conducting an investigation in flight using the "flying wind tunnel"

concept, wherein an aircraft is used as a carrier vehicle for an experiment, can avoid some or all of the above noted wind tunnel limitations, while maintaining operational costs that are competitive with those of wind tunnels.

Some excellent generic research investigations have been previously conducted in flight, including those documented in Refs. 2 to 5. To meet the continuing need to conduct such investigations in flight using the concept of an aircraft for a carrier vehicle, the Dryden Flight Research Facility (DFRF) has modified an F-104G aircraft to carry a low aspect ratio fin on the underside of the fuselage. This fin, commonly referred to as the flight test fixture (FTF), was originally built in the 1960's for panel flutter studies, but has evolved into present use for aeronautics investigations in such areas as skin friction drag, base drag, shuttle tile airloads, and aeronautic instrument development. The fin has its own air data system for determination of FTF reference parameters such as Mach number, altitude, and dynamic pressure. It also contains its own independent instrumentation system, which is primarily oriented towards aerodynamic measurements. Mach numbers of 0.4 to 2.0, dynamic pressures of over 90 kPa (1900 psf), and unit Reynolds numbers of approximately 6.6×10^6 per m (2.0×10^6 per ft) to 23.0×10^6 per m (7.0×10^6 per ft) are achievable with the F-104G/FTF combination.

This report describes the F-104/FTF facility, its capabilities, and past and proposed uses. The operating envelope in terms of Mach number, dynamic pressure, and Reynolds number is discussed. The flow environment on the FTF is shown in terms of chordwise pressure distributions, boundary layer thickness characteristics, and tuft photographs. While it is recognized that many aerodynamic and fluid mechanics experiments require ground-based wind tunnel facilities, examples of experiments that are enhanced or made possible by the capabilities of the FTF are provided.

Flight Test Fixture Description

General Description

The flight test fixture is a low aspect ratio fin-like shape which is mounted vertically on the underside of the F-104G carrier aircraft, with its longitudinal axis aligned along the aircraft's lower fuselage centerline (Figs. 1 and 2). The chord length is 203 cm (80 in.), the semispan is 61 cm (24 in.), and for the major part of its length, except the forebody, the thickness is a constant 16.3 cm (6.4 in.).

The FTF is constructed primarily of aluminum and has a nominal weight of 136 kg (300 lb).

Originally designed to conduct panel flutter tests, the FTF was modified and instrumented to conduct aeronautic investigations, generally related to local flow aerodynamics. The FTF can be flown readily in two symmetrical cross-sectional configurations: (1) the basic FTF shape with a sharp leading edge (wedge forebody), and (2) the radiused forebody incorporating the front portion of a symmetrical supercritical airfoil (the purpose of which is to reduce the

shock strength on the FTF transonically). Both cross sections are shown in Fig. 3. Configurations are changed by an easily removed and installed noseshape.

Instrumentation

The FTF uses a pulse code modulation (pcm) system for data acquisition. The pcm is capable of multiplexing 40 channels at a maximum frequency response of 80 Hz. During flight, data from the pcm are transmitted to the ground via telemetry, as well as being recorded by an onboard recorder. Signals that exceed the 80-Hz limit of the pcm are recorded by the onboard recorder and can be played back after the flight for analysis.

A pitot-static probe, mounted on a boom extending from the forward portion of the FTF (Fig. 2), provides air data measurements for the FTF. The boom is canted 3° nose down in an attempt to minimize misalignment of the probe with the local streamlines during aircraft trim angle-of-attack conditions.

The FTF is equipped with flush static pressure orifices for measurement of chordwise and spanwise pressure distributions, and boundary layer rakes for measurement of boundary layer profiles. Flush static pressure orifices are located on both sides of the FTF. The locations of the orifices are shown in Fig. 4 and listed in Table 1.

Boundary layer rakes can be mounted on both the left and right sides of the FTF. The rakes can be positioned where needed, but are indicated in Fig. 4 at a typical location of approximately the 90-percent chord and midspan of the FTF. Details of the rake geometry are shown in Fig. 5 and listed in Table 2.

Pressure measurements for both pressure distributions and boundary layers were obtained by a 48-port Scanivalve and two other individual differential pressure transducers. The Scanivalve and individual pressure transducers are referenced to FTF boom static pressure, which is measured by a precision absolute pressure transducer. It should be noted that the use of a Scanivalve (one transducer) eliminates bias error between pressure measurements (for example, between different probes on the rakes or between the left and right side of the FTF). This single transducer provides a great amount of precision where incremental boundary layer differences between different surfaces require definition.

For the data presented with forced transition, transition was obtained using No. 36 nominal 0.650-mm (0.026-in.) diameter carborundum grains bonded to the surface of the FTF with plastic adhesive in vertical strips 1.27 cm (0.5 in.) wide. Flow visualization from tufts was provided by short lengths of parachute cord attached to the sides of the FTF with tape.

The F-104G aircraft has an independent instrumentation system which is not discussed in this paper, with the exception of the aircraft flight trajectory guidance system. The key element of this guidance system is a special cockpit display (Fig. 6), which is part of an integrated system that provides the pilot with flight trajectory guidance.[6] The trajectory guidance system uplinks engineering parameters calculated on a ground-based computer (using aircraft or FTF telemetry, or both) to the cockpit display

in real time. In Fig. 6, the four display indicators are noted. The vertical needle is typically used for bank error during constant Mach, alpha, and altitude turns. The horizontal needle can be used for Reynolds number error, and the turn needle is normally used for FTF 0° sideslip error. The speed bug is normally used for Mach number error.

Description of FTF Flow Environment

Pressure distribution data and boundary layer characteristics have been obtained for both the basic FTF wedge forebody and the symmetrical supercritical noseshape (radiused forebody). Pressure transducers sensing local pressures from mirror image locations on both sides of the FTF provide an excellent source of real-time data (by means of the uplink display) for the pilot to determine when the FTF sideslip angle is zero. Data presented herein were obtained at zero sideslip on the FTF, which implies the same flow field on both sides of the FTF. Consequently, data discussions in this section apply to both sides of the FTF.

Figure 7 presents FTF chordwise pressure distributions on the left and right side leading edge, and base pressures for the wedge forebody configuration and the symmetrical supercritical noseshape (radiused forebody) at selected FTF Mach numbers of 0.57, 0.86, and 1.22. For simplification, only pressure data on the left side centerline of the radiused forebody are presented. The data at $x/c = 1.00$ are base pressure coefficients, which are presented as reference for base drag experiments.

For the wedge forebody (triangle symbols), the negligible difference in pressure coefficient (C_p) between the left and right side leading edge ($x/c = 0$ to 0.15) indicates that the FTF is at a sideslip of 0°. At an FTF Mach number of 0.86 (Fig. 7(b)), a peak occurs in the pressure distribution at approximately 20-percent chord. The pressure coefficient level of the peak exceeds the critical level (C_p^*) and terminates in an abrupt increase in pressure, which indicates the presence of a normal shock.

For the symmetrical supercritical nose, radiused forebody (circle symbols), the shape of the pressure distribution near the leading edge is much different and more negative in level than the data for the wedge forebody. Similarly, in Fig. 7(b) ($M_{FTF} = 0.86$), the data for the radiused forebody exceeds the critical level (C_p^*) and terminates in an abrupt increase in the pressure at approximately 15- to 20-percent chord, which also indicates the presence of a normal shock. However, this abrupt increase in pressure is smaller in magnitude than that indicated in the data for the wedge forebody. This demonstrates the expected reduced strength of the normal shock for the symmetrical supercritical noseshape, radiused forebody.

Figure 8 presents spanwise variation of pressure coefficient at $x/c = 0.67$ for both the basic FTF wedge forebody and the symmetrical supercritical noseshape. Data are presented for a transonic ($M = 0.86$) and a supersonic ($M = 1.22$) case. In Fig. 8(a), spanwise pressure distribution is virtually constant at the transonic Mach number presented. In Fig. 8(b),

at an average supersonic Mach number of 1.22, the data for the basic FTF wedge forebody show a spanwise variation of approximately 0.15 pressure coefficient, while no variation is noted for the symmetrical supercritical noseshape. These spanwise variations of pressure are considered negligible, indicating a quasi-two-dimensional environment for both forebody configurations.

Figure 9 presents boundary layer displacement thickness (δ^*) versus FTF Mach number for both the wedge nose and the symmetrical supercritical noseshape, with transition fixed at 7.5 and 5.0 percent, respectively. The data show that the symmetrical supercritical noseshape decreases the displacement thickness transonically ($M_{FTF} = 0.65$ to 0.93) relative to the wedge forebody. Both forebody configurations show trends of increased displacement thickness as $M_{FTF} = 0.80$ is approached, which corresponds to the Mach numbers which show evidence of normal shock formation in the pressure data of Fig. 7. The scatter in the data near $M_{FTF} = 0.80$ (for both forebodies) is attributed to boundary layer instabilities caused by the normal shock formation.

Figure 10 shows representative in-flight tuft photographs for the wedge nose configuration at transonic and supersonic FTF Mach numbers of 0.85 and 1.13, respectively. In Fig. 10(a) at an FTF Mach number of 0.85, some unsteadiness is indicated in the second column of tufts ($x/c = 0.30$). The unsteadiness is probably the result of the upstream normal shock wave noted earlier from pressure distribution and boundary layer thickness data. Otherwise, the tufts appear stable and aligned straight back. In Fig. 10(b) at an FTF Mach number of 1.13, the tufts appear stable and aligned straight back. The straight-back appearance of the tufts in Figs. 10(a) and 10(b) are indicative of quasi-two-dimensional flow and agree with the previously noted negligible variation of spanwise pressure in Fig. 8.

F-104/FTF Capabilities

Envelope

The F-104/FTF facility has some unique operational envelope capabilities with respect to wind tunnels. These capabilities include a larger Mach number, Reynolds number, and dynamic pressure envelope than most wind tunnels, and the capability for testing large or full-scale test articles. Additionally, data can be obtained on the FTF near and through a Mach number of 1.0 with little or no adverse effects. For comparison, Figs. 11 and 12 present Reynolds number and dynamic pressure versus Mach number envelopes for the F-104/FTF and the NASA Ames 11-Foot Transonic Wind Tunnel.[1] The Ames 11-foot wind tunnel is used for comparison because it has one of the largest envelopes of any transonic wind tunnel.

Figure 11(a) presents unit Reynolds number envelopes for the F-104/FTF and the Ames 11-foot wind tunnel. The wind tunnel has unit Reynolds number advantages over the FTF; however, the F-104/FTF has a much larger Mach envelope than the wind tunnel ($M = 0.4$ to 2.0 for the F-104/FTF compared to $M = 0.5$ to 1.4 for the Ames 11-Foot Transonic Wind Tunnel).

At least two separate wind tunnel facilities would be required to span the Mach number envelope of the F-104/FTF. The Mach number gap in the Ames 11-foot wind tunnel envelope represents the area near a Mach number of 1.0, where it is normally difficult to obtain reliable data in a wind tunnel.

Figure 11(b) compares Reynolds number envelopes for the two facilities, based on representative test specimen chord lengths. These chord lengths might be representative of airfoil tests, for example. The wind tunnel envelope is based on a test specimen chord of 0.61 m (2 ft), which was felt to be representative of a test article that could be tested throughout the Mach number range presented (M = 0.5 to 1.4), and the FTF envelope is based on the 2.0-m (80-in.) chord of the FTF. For this example, the F-104/FTF shows significantly more Reynolds number capability than the wind tunnel. For example, at a Mach number of 0.8, the F-104/FTF is capable of a Reynolds number of 40 million, which is representative of a large transport aircraft. This example points out the potential capability of the F-104/FTF to greatly exceed the capability of wind tunnels when large chord Reynolds numbers are desired.

Figure 12 presents the dynamic pressure ($\bar{q}$) versus Mach number envelope for the F-104/FTF and the Ames 11-Foot Transonic Wind Tunnel. The figure indicates a slightly higher maximum dynamic pressure capability in the wind tunnel, but for a much smaller range of Mach number. However, large or full-scale test articles may cause blockage of the wind tunnel circuit and lower the dynamic pressure capability by as much as half the values indicated. Blockage constraints do not, of course, limit the dynamic pressure envelope of the F-104/FTF.

Flight Guidance and Trajectories

The F-104/FTF facility is equipped with a special cockpit display (Fig. 6), which is part of an integrated system that provides the pilot with flight trajectory guidance.[6] This system results in significant improvement in the accuracy and speed with which pilots approach and maintain desired flight test conditions or trajectories. The result is that some unique trajectories are routinely flown, including constant Reynolds number profiles for fluid mechanics experiments (such as skin friction), dynamic pressure versus Mach number profiles for airload tests, and constant Mach number, altitude, and angle-of-attack turns for performance tests.

Figure 13 presents an example of the type of trajectories and the accuracy with which they can be flown. The two horizontal lines represent constant Reynolds numbers of 6.6×10^6 per m (2.0×10^6 per ft) and 16.4×10^6 per m (5.0×10^6 per ft). Plotted along with these lines are flight data obtained using uplink for trajectory guidance to fly these desired values of unit Reynolds number. Another possible trajectory is shown by the vertical line, which represents a constant Mach number trajectory while varying Reynolds number.

The uplink is also used, as was mentioned earlier, to maintain a zero sideslip condition on the FTF during fluid mechanics experiments.

Typical Experiments

This section presents typical experiments which have been conducted or are proposed to be conducted on the FTF. Experiments that are enhanced by the unique capabilities of the F-104/FTF are noted.

Base Drag

The blunt base of the FTF (8 percent of the chord) has been used to conduct experiments for the reduction of base drag at subsonic and transonic speeds. The fin-like blunt base configuration of the FTF is considered to be representative of present and future blunt-based fuselages and blunt trailing-edged stabilizing surfaces of reentry or hypersonic vehicles. Reference 7 describes and discusses an early use of the FTF for determining, in flight, the effectiveness of splitter plates in reducing base drag at subsonic speeds and high chord Reynolds numbers. Figure 14 shows rear views of the dismounted FTF with the blunt base, splitter plate, and vented cavity configurations, and data from Ref. 8, which documents an experiment conducted more recently than that in Ref. 7.

Reference 7 notes that the increment in base pressure coefficient for the splitter plate is very similar to the increments obtained on a two-dimensional wind tunnel model, even though the flight results represented higher Reynolds numbers and contained three-dimensional effects (an outboard end). Other base pressure data obtained from the FTF are reported in Ref. 9.

The FTF provides a capability to conduct experiments on a full-scale, blunt base, fin-like configuration at Mach numbers from 0.4 to 2.0 and at high Reynolds numbers. Additionally, the capability to conduct representative base drag reduction experiments has been demonstrated.

Instrument Evaluation

The independent instrumentation system and well documented flow field of the FTF make it a useful test bed for flight instrumentation evaluation and development. Both traversing and pivoting traversing boundary layer probes have thus far been evaluated, and several airspeed probes are proposed for evaluation using the FTF.

The pivoting traversing boundary layer probe evaluation is discussed in Ref. 10. The device, shown in Fig. 15(a), was mounted on the right side of the FTF about midspan at the 60-percent chord. The pivoting probe was a derivative of the screw-driven traversing probes reported in Ref. 11, except that the pitot element was allowed to pivot into the local airstream as well as traverse the boundary layer. The unit successfully measured simultaneously flow angularity, probe height, and pitot pressure through the boundary layer. Figures 15(b) and 15(c) show typical results obtained with the traversing probe.[11]

References 12 and 13 describe unique air data probes, primarily intended for use at supersonic speeds. One is referred to as a share-plow probe (Fig. 16) and the other as a shock-swallowing probe (Fig. 17). The intent of both probes is to measure

true total pressure at supersonic speeds, p_{t_1}, rather than the usual total pressure behind the shock, p_{t_2}.

It has been proposed that the existing pitot-static probe on the FTF be replaced by these unique air data probes. This would provide a unique capability to conduct an in-flight operational evaluation of these probes at both supersonic and subsonic speeds without interfering with the aircraft (pilot's) system. It would also provide an in-flight calibration for comparison to existing wind tunnel data.

Shuttle Tile Airload Tests

To contribute to the certification of the structural integrity of the space shuttle orbiter's thermal protection system before the first shuttle flight (April 1981), in-flight and wind tunnel aerodynamic load tests of several simulated local areas of the orbiter surface were conducted. Flight tests of six areas are described in Ref. 5. One simulated area, the elevon cove (Fig. 18), was tested on the FTF. The FTF was used for this test because of (1) the capability to expose actual full-scale shuttle tiles to realistic airloads, (2) the large Mach number/dynamic pressure envelope of the carrier aircraft, (3) the ability to obtain data near and through a Mach number of 1.0, and (4) the ability to respond quickly to the requirements of the test.

The launch profiles shown in Fig. 19 were flown for this test article. The maximum airload on the orbiter elevon cove area was predicted to occur at a Mach number of 1.1.

Figure 20 presents pressure coefficient data along the longidudinal axis of the test article (which corresponds to chordwise on the orbiter) at a Mach number of 1.1. The general trends (slopes) of the F-104 flight data agree well with the orbiter design data; however, the levels are displaced. The slope $\dfrac{\Delta C_p}{\Delta(x/c)}$ was considered the important parameter to match on this test article to correctly simulate airloads, and the match of these slopes was considered good.

Exposure of the test article to the pressure simulations at 1.4 times the design dynamic pressure showed no major deficiencies of the orbiter elevon cove TPS.

Several similar full-scale articles were tested in various wind tunnels. In those tests, the launch profile dynamic pressures shown in Fig. 19 were normally not achieved, because the large size of the test articles severely blocked the wind tunnel circuit. The FTF provided a unique capability to test a "full-scale" test article to the desired combinations of dynamic pressure and Mach number. Additionally, the F-104/FTF provided the capability to test the articles through a complete M versus q profile, rather than testing discrete points as was normally done in the wind tunnel tests.

Skin Friction

The large chord, ability to change forebody configurations (pressure distribution), large Mach/Reynolds number envelope, and profile capability (via uplink), such as a constant Reynolds number profile, make the FTF a unique facility for conducting skin friction experiments. DFRF is currently developing a large force balance (Fig. 21) to be installed flush on the sides of the FTF at about 80-percent chord. This will allow the direct measurement of skin friction with the force balance and concurrent determination of skin friction from boundary layer measurement using existing rakes.

The proposed skin friction experiments would place excrescencies such as rivet heads, fasteners, and different paint finishes on one side of the FTF while the other side would be maintained as a clean and smooth "control." By flying the FTF at 0° sideslip, both the experiment and control sides could be exposed to the same flow environment simultaneously.

Concluding Remarks

During the 1960's, an F-104 aircraft was modified to carry a low aspect ratio fin on the underside of the fuselage for the purpose of conducting panel flutter tests in a flight environment. This test fixture has evolved into a versatile facility for the conduct of aerodynamics and fluid mechanics research.

The aircraft/test fixture combination has demonstrated a capability for a wide variety of aerodynamics and fluid mechanics experiments over a Mach number range extending from 0.4 to 2.0 and a chord Reynolds number of over 40×10^6. This combination is also characterized by an ability to respond quickly to the requirements of a test and by operational costs which are competitive with or less than comparable ground facilities.

Other characteristics of this facility are as follows:

1. The facility is capable of testing full-scale test articles, which are potentially larger than those that can be tested in wind tunnels.

2. With the use of uplink, unique trajectories, such as constant Reynolds number profiles, can be flown routinely.

3. Reliable data can be obtained through the transonic region, including Mach 1.0.

4. Small increments in friction drag between two test surfaces can be defined.

5. Representative base drag reduction experiments can be conducted.

6. Pressure distributions can be changed easily with interchangeable noseshapes.

References

[1] Pirrello, C. J., Hardin, R. D., Heckart, M. V., and Brown, K. R., "An Inventory of Aeronautical Ground Research Facilities, Volume I—Wind Tunnels," NASA CR-1874, 1971.

[2] Quinn, Robert D., and Gong, Leslie, "In-Flight Boundary-Layer Measurements on a Hollow Cylinder at a Mach Number of 3.0," NASA TP-1764, 1980.

[3]Stallings, Robert L., Jr., and Lamb, Milton, "Wind-Tunnel Measurements and Comparison With Flight of the Boundary Layer and Heat Transfer on a Hollow Cylinder at Mach 3," NASA TP-1789, 1980.

[4]Dougherty, N. S., Jr., and Fisher, D. F., "Boundary-Layer Transition on a 10-Deg Cone: Wind Tunnel/Flight Correlation," AIAA Paper 80-0154, Jan. 1980.

[5]Meyer, Robert R., Jr., Jarvis, Calvin R., and Barneburg, Jack, "In-Flight Aerodynamic Load Testing of the Shuttle Thermal Protection System," AIAA Paper 81-2468, Nov. 1981.

[6]Swann, M. R., Duke, E. L., Enevoldson, E. K., and Wolf, T. D., "Experience with Flight Test Trajectory Guidance," AIAA Paper 81-2504, Nov. 1981.

[7]Saltzman, Edwin J., and Hintz, John, "Flight Evaluation of Splitter-Plate Effectiveness in Reducing Base Drag at Mach Numbers From 0.65 to 0.90," NASA TM X-1376, 1967.

[8]Pyle, Jon S., and Saltzman, Edwin J., "Review of Drag Measurements From Flight Tests of Manned Aircraft With Comparisons to Wind-Tunnel Predictions," AGARD Specialists' Meeting of Fluid Dynamics Panel, Izmir, Turkey, Apr. 10-13, 1973.

[9]Saltzman, Edwin J., and Bellman, Donald R. "A Comparison of Some Aerodynamic Drag Factors Determined in Full-Scale Flight With Wind-Tunnel Theoretical Results," AGARD Specialists' Meeting Facilities and Techniques for Aerodynamic Testing Transonic Speeds and High Reynolds Numbers, Göttingen, Germany, Apr. 26-28, 1971.

[10]Montoya, Lawrence C., Brauns, David A., Cissel, Ralph E., "Flight Experience With a Pivoti Traversing Boundary-Layer Probe," NASA TM X-56022, Jan. 1974.

[11]Saltzman, Edwin J., "In-Flight Use of Trave ing Boundary-Layer Probes," NASA TN D-6428, 1

[12]Couch, Lana M., "Effects of Geometric Varia on the Performance of a Probe for Direct Measurem of Free-Stream Stagnation Pressure in Supersonic Flow," NASA TN D-7887, 1975.

[13]Nugent, Jack, Couch, Lana M., and Webb, Lannie D., "Exploratory Wind Tunnel Tests of a Shock-Swallowing Air Data Sensor at a Mach Numb of Approximately 1.83," NASA TM X-56030, 1975.

TABLE 1.—FTF ORIFICE LOCATIONS
(ℓ, left side; r, right side; b, base)

(a) Basic FTF, wedge forebody

x/c	y/c	Location
0.047	0.558	ℓ, r
0.094		ℓ, r
0.123		r
0.144		ℓ, r
0.213		ℓ
0.275		
0.337		
0.412		
0.487		
0.562		
0.637		
0.675	0.313	
0.675	0.438	
0.675	0.558	
0.675	0.684	
0.675	0.808	
0.713	0.558	
0.787		
0.863		
0.937		
1.000	0.276	b
1.000	0.445	
1.000	0.612	
1.000	0.781	

TABLE 1.—Concluded

(b) Symmetrical supercritical, radiused forebod

x/c	y/c	Location
0.020	0.558	ℓ
0.040		
0.080		
0.120		
0.160		
0.222		
0.272		
0.333		
0.407		
0.481		
0.555		
0.625		
0.667	0.313	
0.667	0.438	
0.667	0.558	
0.667	0.684	
0.667	0.808	
0.704	0.558	
0.777		
0.852		
0.925		
1.000	0.276	b
1.000	0.445	
1.000	0.612	
1.000	0.781	
0	0.779	ℓ
0.020		
0.040		
0.080		
0.020	0.338, 0.779	r
0.040		
0.080		
0.120		
0.160		

TABLE 2.—BOUNDARY LAYER RAKE PROBE HEIGHT

Rake number	h, cm(in.)
1	0.104(0.041)
2	0.318(0.125)
3	0.531(0.209)
4	0.800(0.315)
5	1.069(0.421)
6	1.339(0.527)
7	1.608(0.633)
8	1.918(0.755)
9	2.228(0.877)
10	2.540(1.000)
11	3.175(1.250)
12	3.810(1.500)
13	4.445(1.750)
14	5.080(2.000)
15	6.350(2.500)
16	7.620(3.000)
17	8.890(3.500)
18	10.160(4.000)
19	11.430(4.500)
20	12.700(5.000)

Flight test fixture

Fig. 1 Flight test fixture installed on lower fuselage of F-104 carrier aircraft.
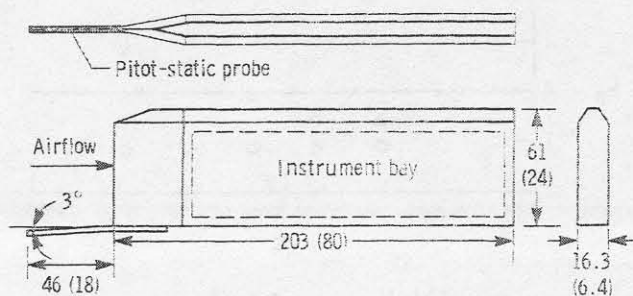
Fig. 2 Flight test fixture with wedge forebody shape. Dimensions in centimeters (inches).
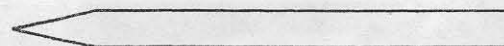
(a) Wedge forebody, basic FTF.

(b) Radiused forebody, modified with forward portion of symmetrical supercritical airfoil.

Fig. 3 Cross sections of presently available FTF forebodies.

o Left side
□ Right side
◇ Base
× Present rake location

(a) Basic FTF, wedge forebody.

o Left side
□ Right side
× Present rake location
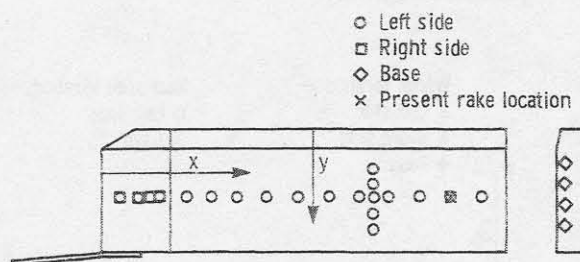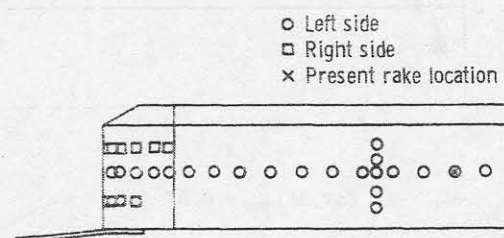
(b) Symmetrical supercritical, radiused forebody.

Fig. 4 Orifice locations for FTF.

Rake 12 Conical head

8.5
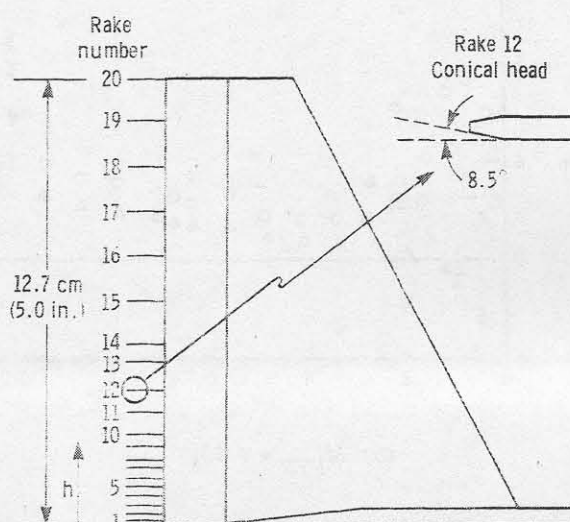
Fig. 5 Boundary layer rake (one on each side).
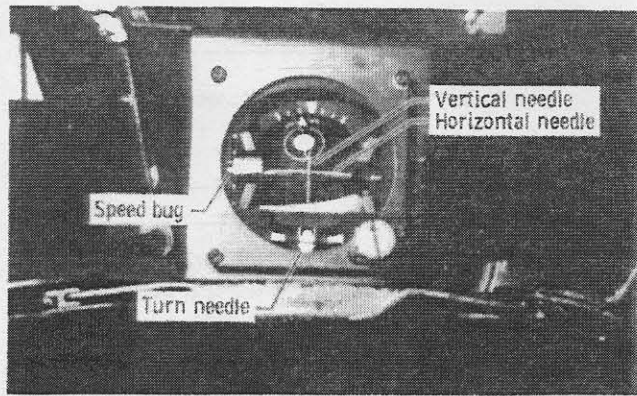
Fig. 6 Cockpit display for flight trajectory guidance, uplink.

(c) $M_{FTF} = 1.22$.

Fig. 7 Concluded.
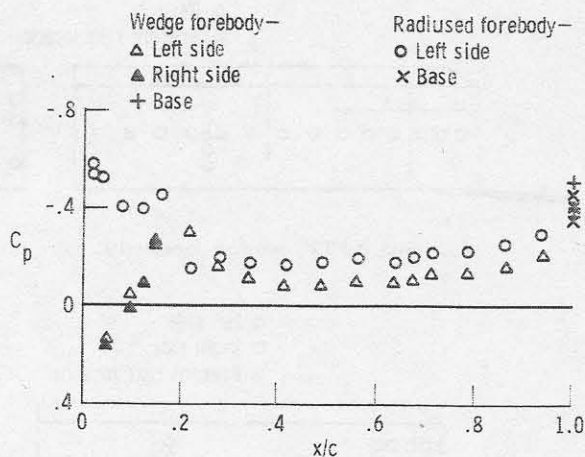
(a) $M_{FTF} = 0.57$.
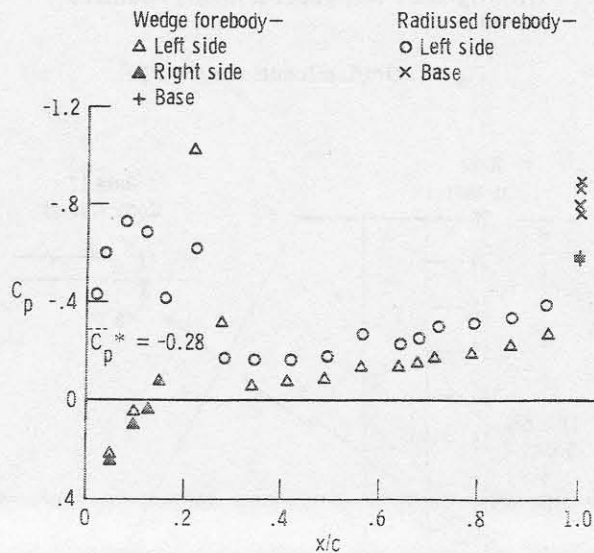
(a) $M_{FTF_{avg}} = 0.86$.

(b) $M_{FTF} = 0.86$.

Fig. 7 Typical FTF cordwise pressure distribution at zero sideslip.
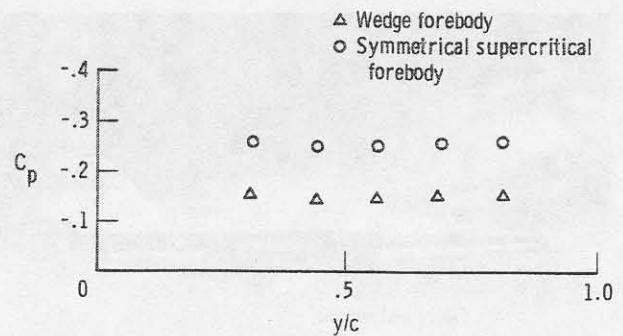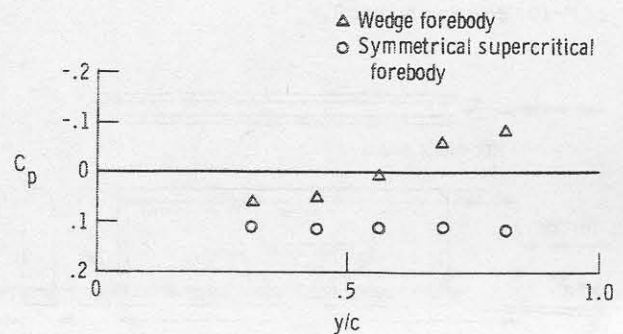
(b) $M_{FTF_{avg}} = 1.22$.

Fig. 8 Spanwise variation of pressure coefficient for both forebody configurations at $(x/c)_{avg} = 0.67$.

8
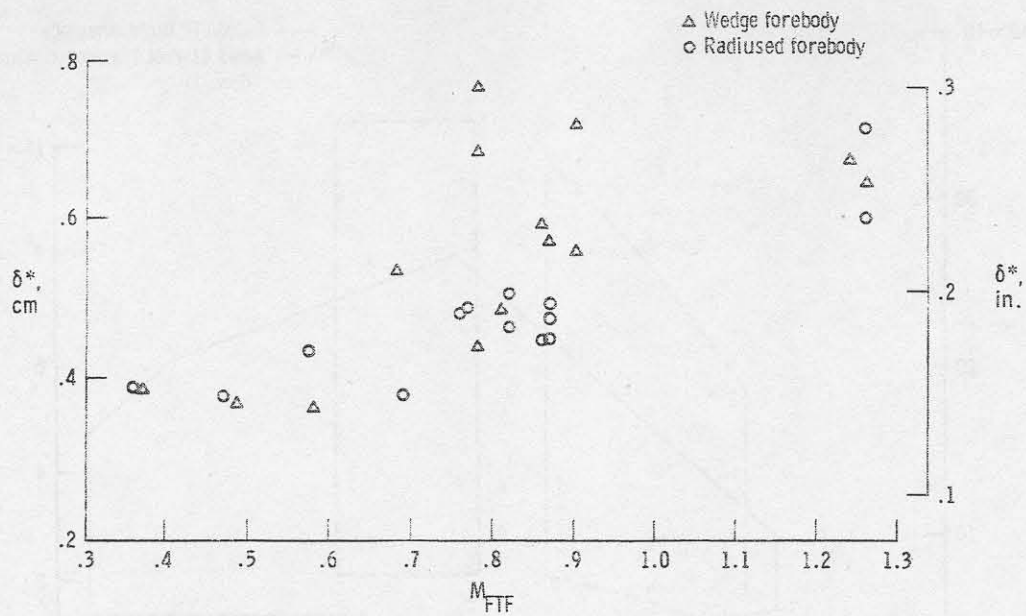
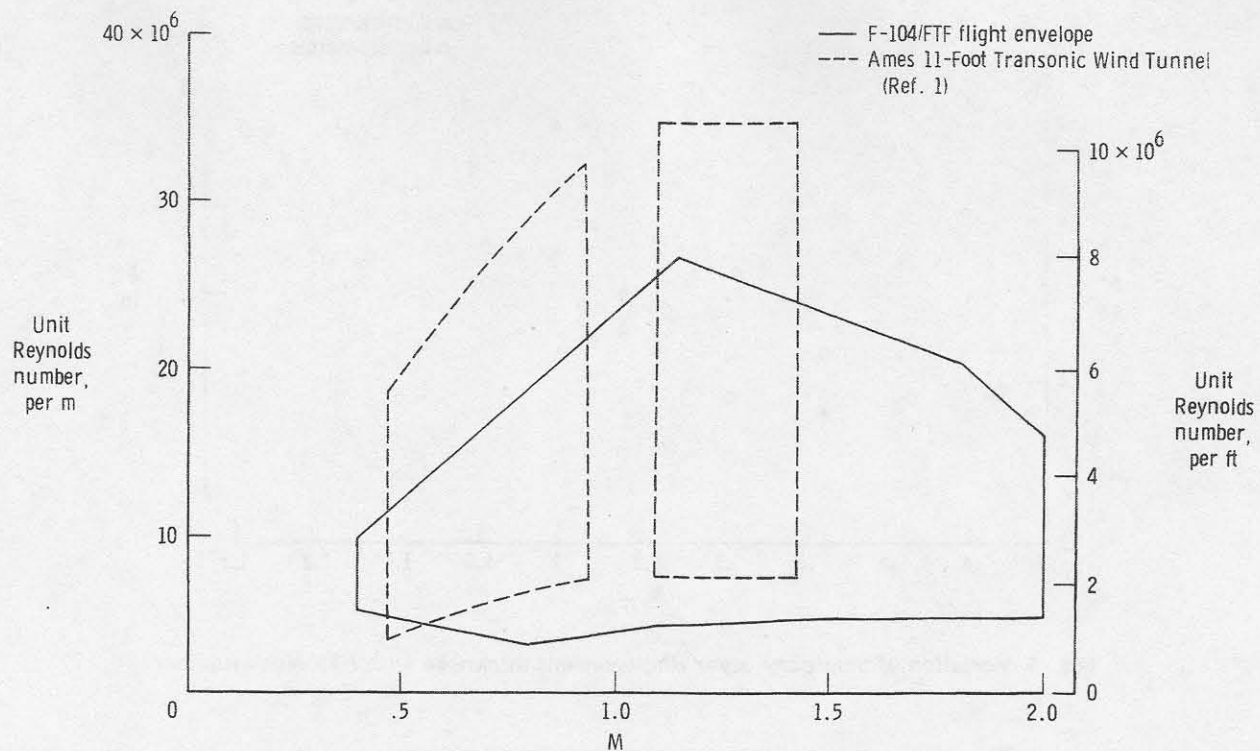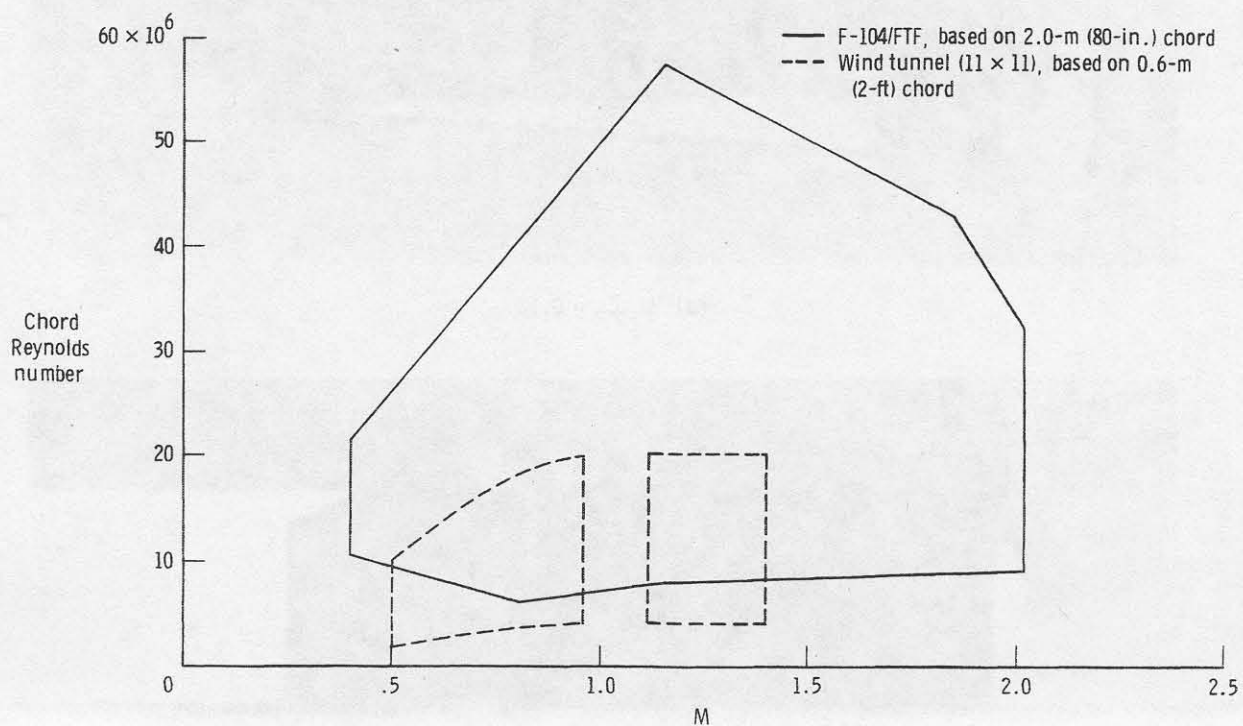Fig. 9 Variation of boundary layer displacement thickness with FTF Mach number.
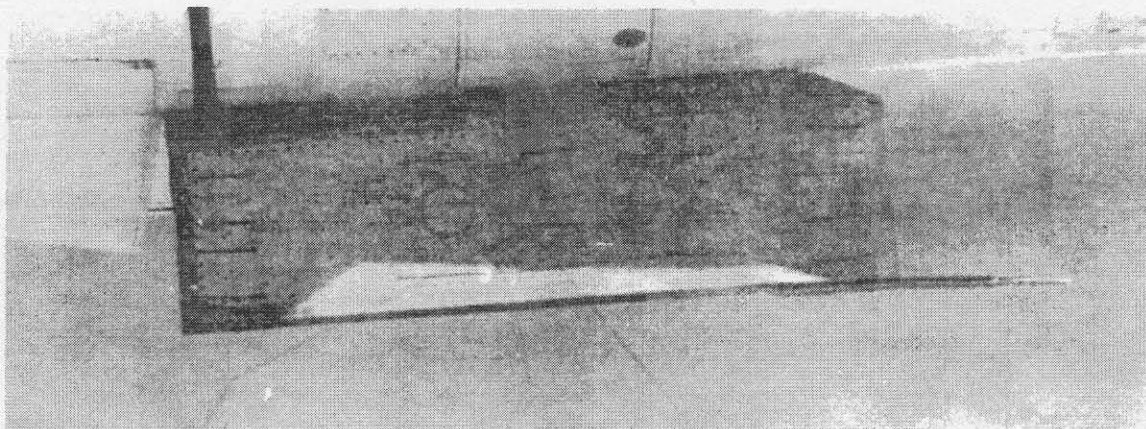
(a) $M_{FTF} = 0.85$.
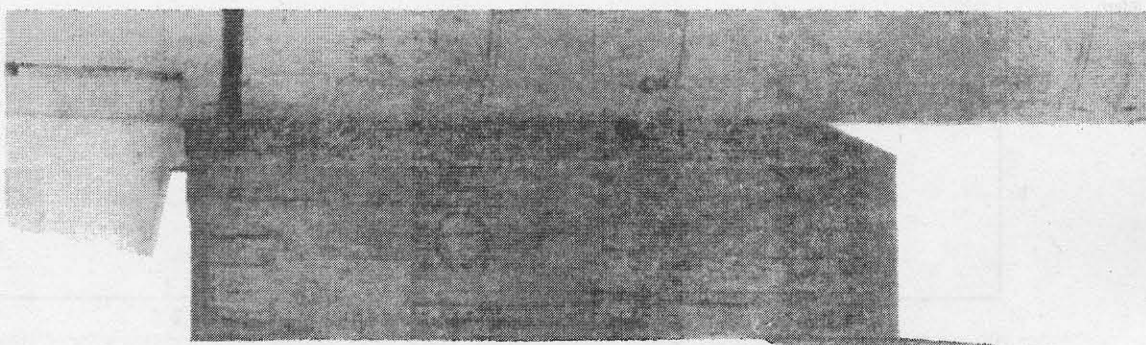
(b) $M_{FTF} = 1.13$.

Fig. 10 Representative in-flight tuft patterns.

9

(a) Unit Reynolds number.

(b) Chord Reynolds number.

Fig. 11 Mach-Reynolds number envelope.
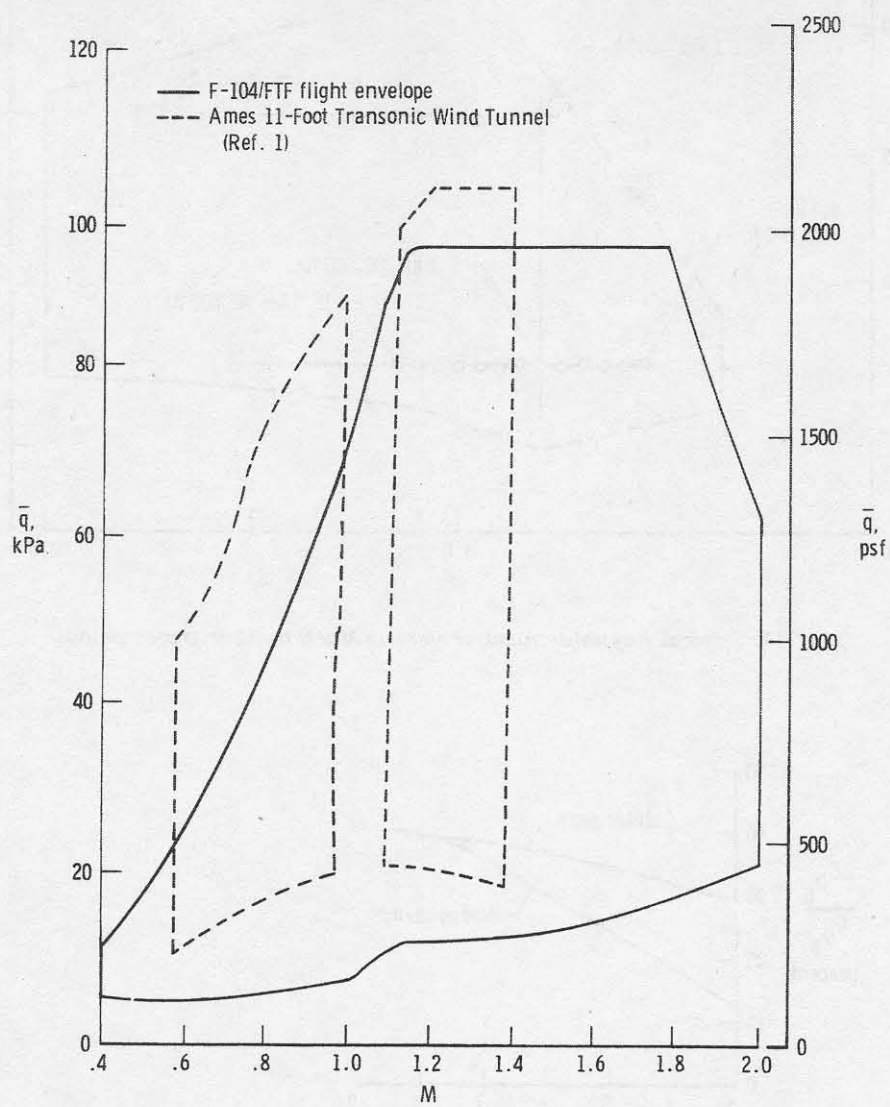
Fig. 12 Mach number/dynamic pressure envelope.
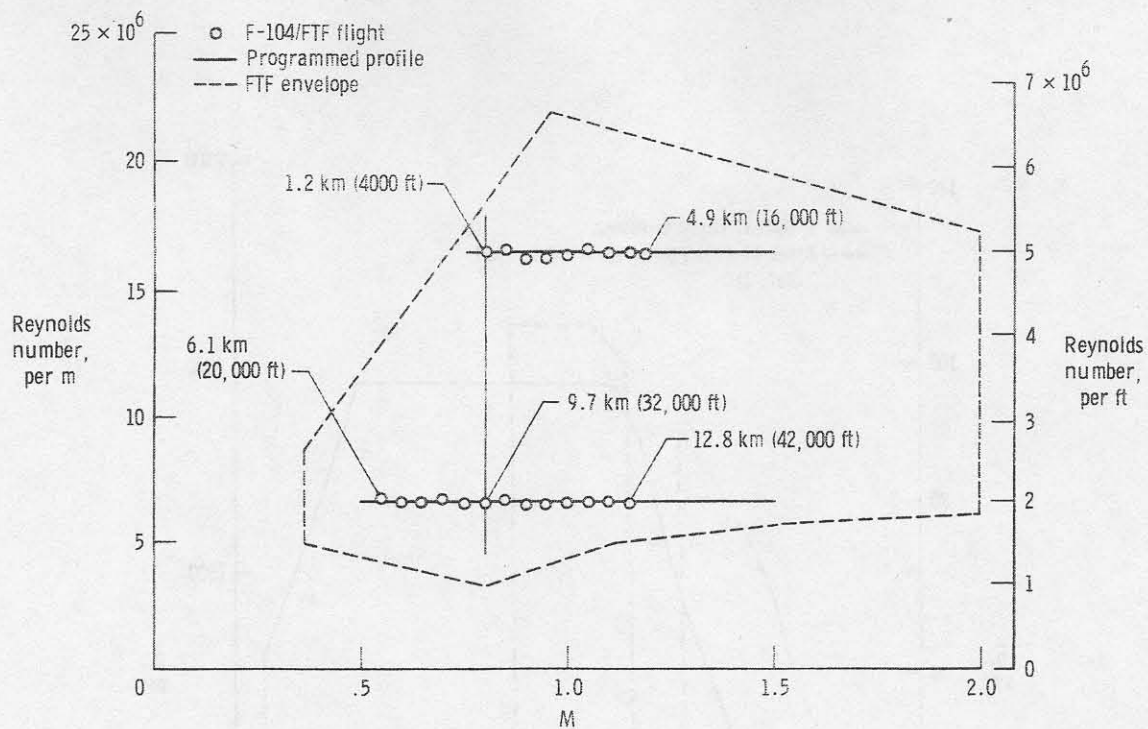
Fig. 13 Typical Reynolds number versus Mach number trajectories.
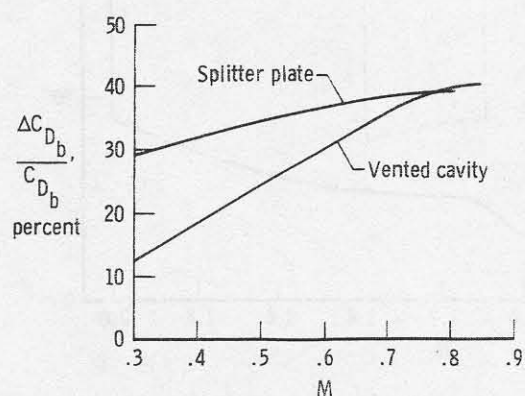
Reduction of base drag on F-104 test fixture using
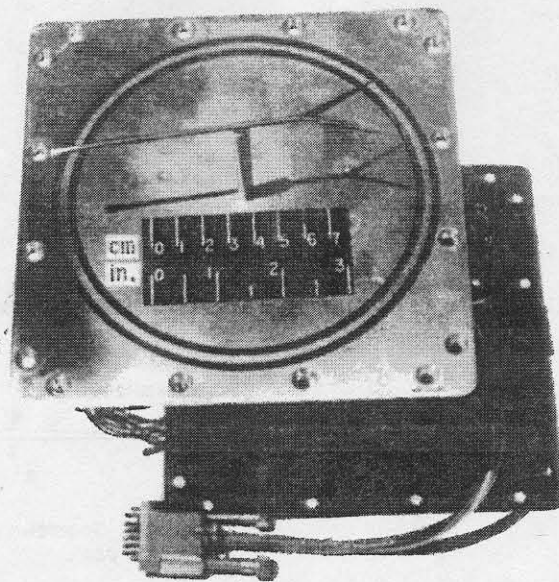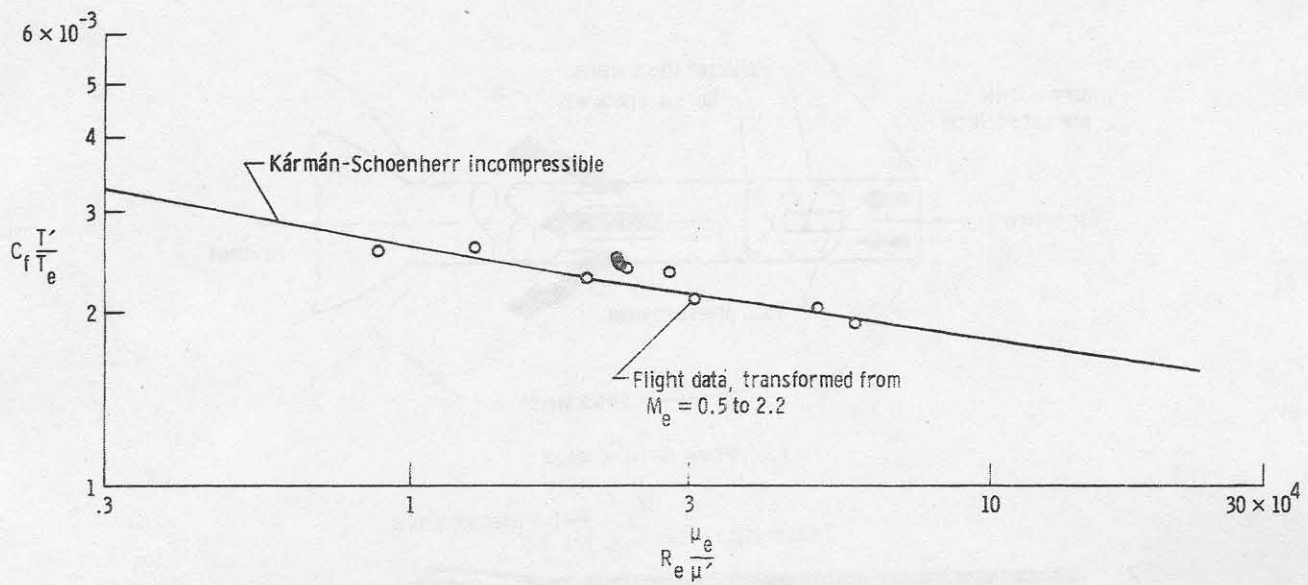splitter plate and vented cavity (Ref. 8).
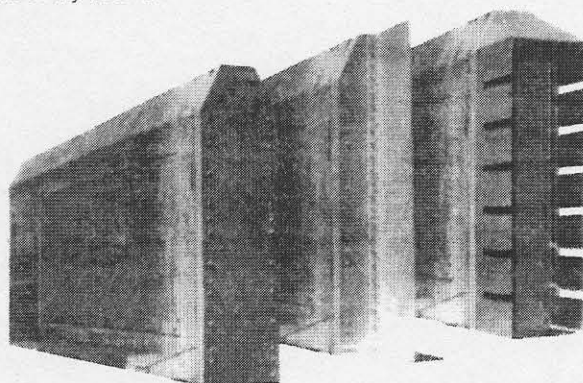
Fig. 14 FTF base configurations tested and results.

(a) Pivoting traversing probe.

$C_f \dfrac{T'}{T_e}$

Kármán-Schoenherr incompressible

Flight data, transformed from
$M_e = 0.5$ to 2.2

$R_e \dfrac{\mu_e}{\mu'}$

(b) Comparison of local friction coefficients derived from traversing probe data (Ref. 11).

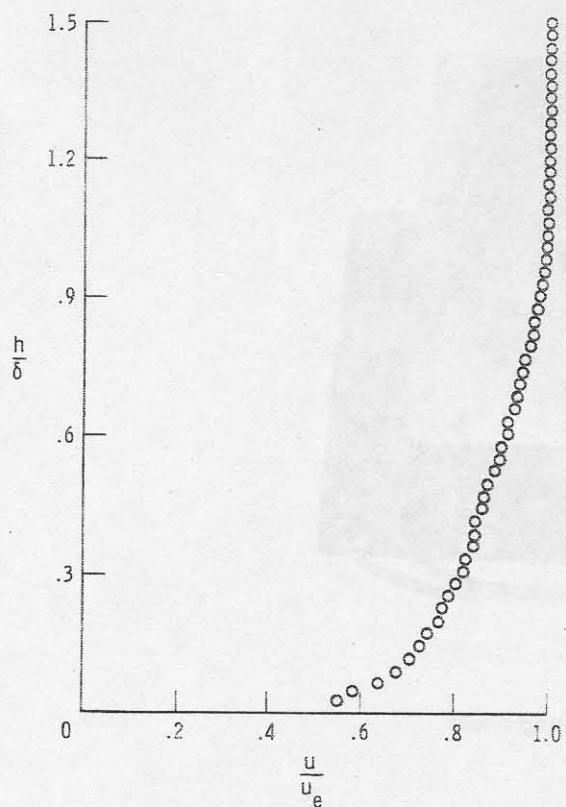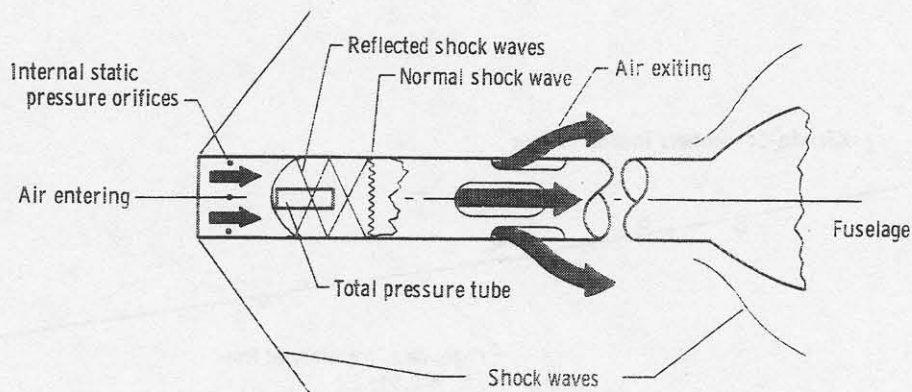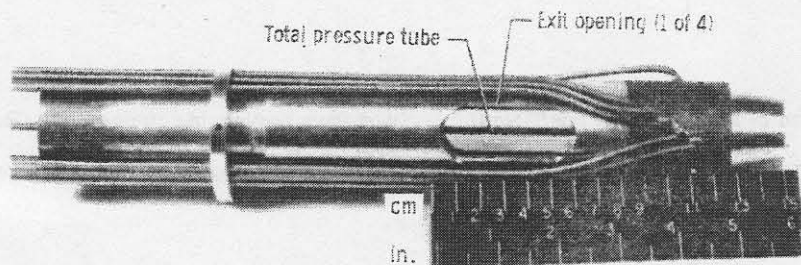Fig. 15 Traversing boundary layer probe demonstrated in Ref. 10.

(c) Conventional velocity ratio profile; single traverse (Ref. 11).
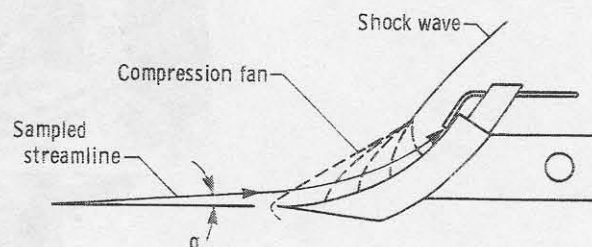
Fig. 15 Concluded.

Fig. 16 Geometry and flow field sketch of share-plow probe.

(a) Flow field sketch.
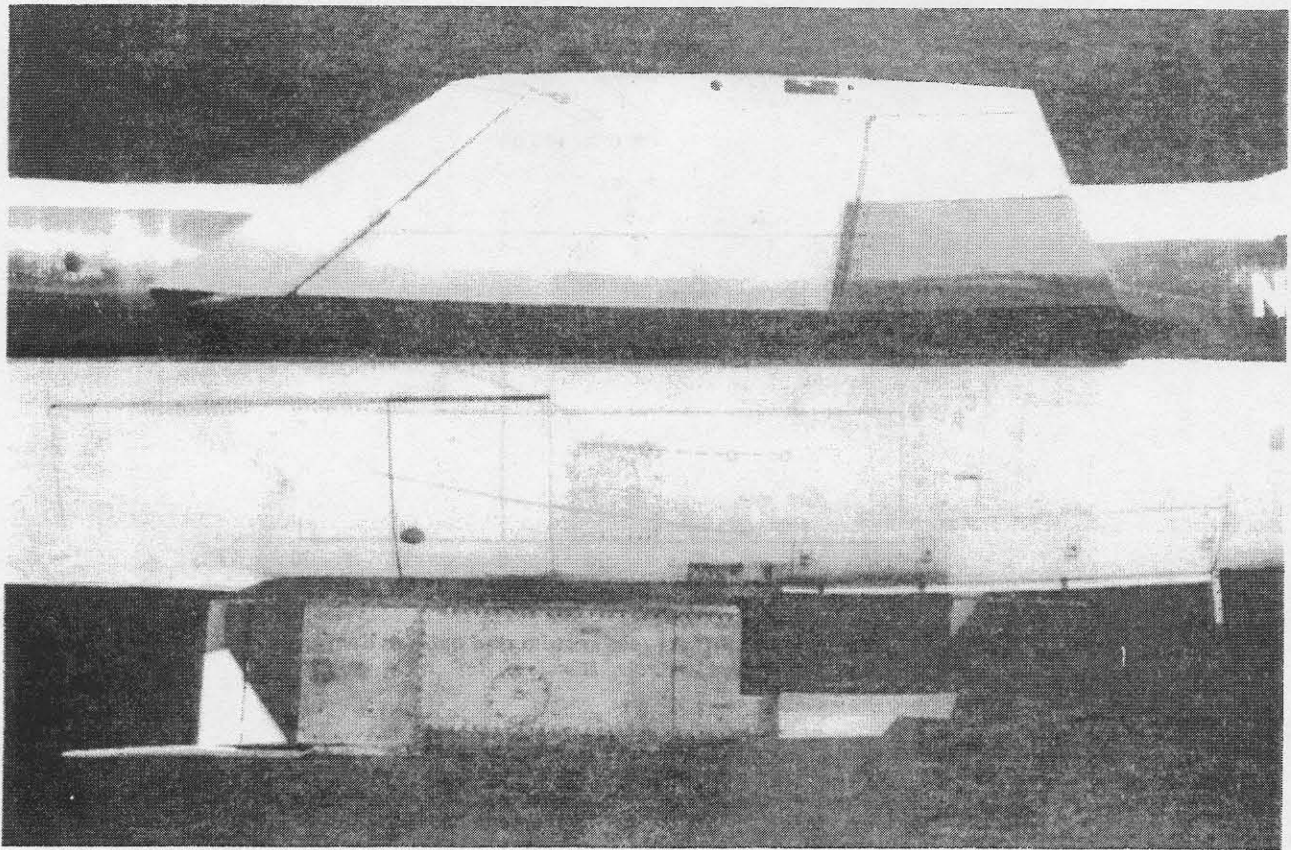

(b) Photograph.

Fig. 17 Shock-swallowing probe.

14

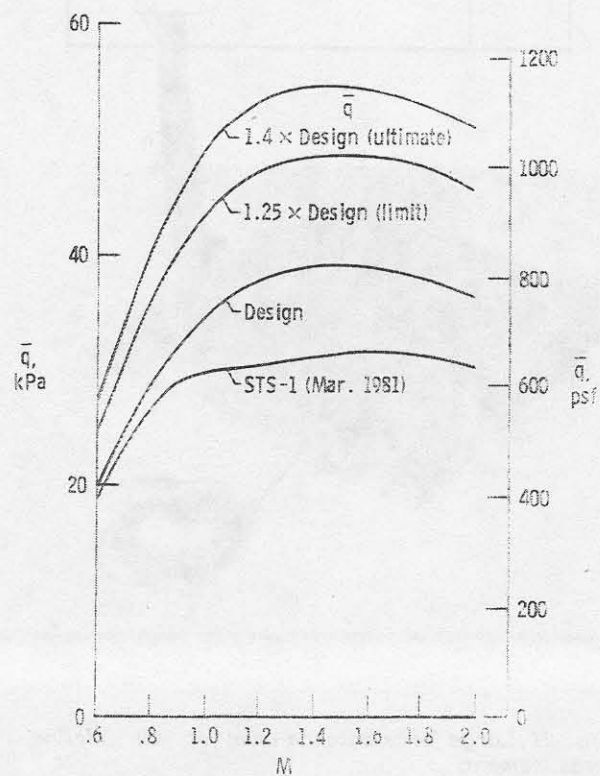Fig. 18 Orbiter elevon cove test article mounted on aft portion of FTF.

Fig. 19 Profiles flown to test TPS elevon cove
test article (Ref. 5).
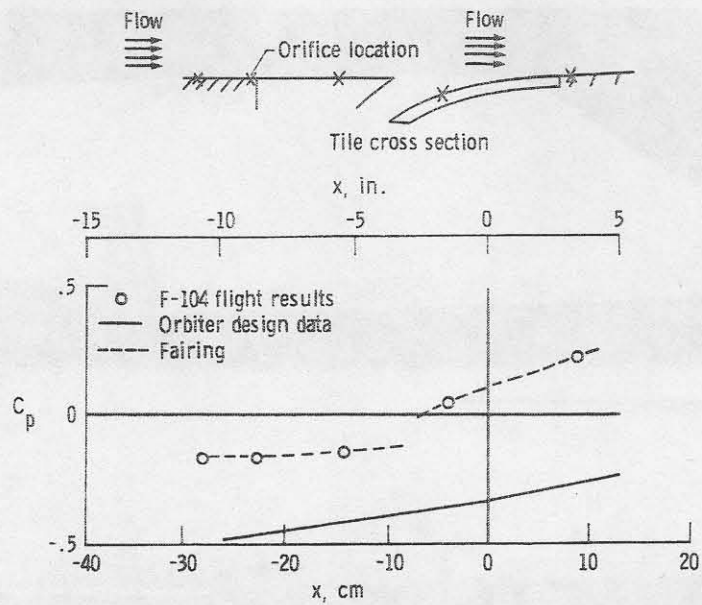
Flow

Orifice location

Flow

Tile cross section

x, in.

Fig. 20 Comparison of flight test results and orbiter design
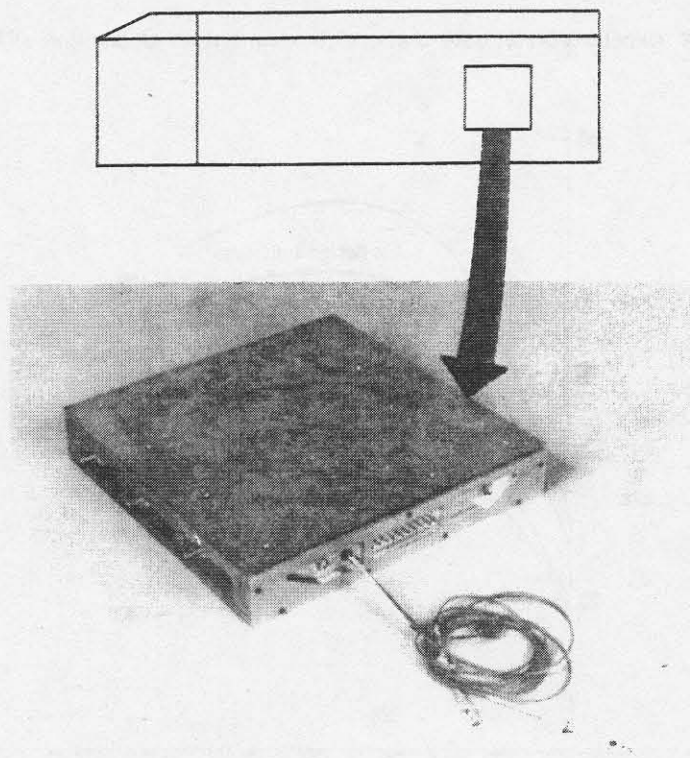data for elevon cove test article. M = 1.1; Ref. 5.

Fig. 21 Large force balance used for skin friction
measurements.

16

1. Report No. NASA TM-84900	2. Government Accession No.	3. Recipient's Catalog No.
4. Title and Subtitle A UNIQUE FLIGHT TEST FACILITY: DESCRIPTION AND RESULTS		5. Report Date November 1982
		6. Performing Organization Code RTOP 505-31-44
7. Author(s) Robert R. Meyer, Jr.		8. Performing Organization Report No.
		10. Work Unit No.
9. Performing Organization Name and Address Ames Research Center Dryden Flight Research Facility Edwards, California 93523		11. Contract or Grant No.
		13. Type of Report and Period Covered Technical Memorandum
12. Sponsoring Agency Name and Address National Aeronautics and Space Adminstration Washington, D.C. 20546		14. Sponsoring Agency Code

15. Supplementary Notes

This paper was presented as ICAS Paper 82-5.3.3 at the 13th Congress of the International Council of the Aeronautical Sciences (ICAS)/AIAA Aircraft Systems and Technology Conference at Seattle, Washington, August 22-27, 1982.

16. Abstract

The Dryden Flight Research Facility has developed a unique research facility for conducting aerodynamic and fluid mechanics experiments in flight. A low aspect ratio fin, referred to as the flight test fixture (FTF), is mounted on the underside of the fuselage of an F-104G aircraft. The F-104G/FTF facility is described, and the capabilities are discussed. The capabilities include (1) a large Mach number envelope (0.4 to 2.0), including the region through Mach 1.0; (2) the potential ability to test articles larger than those that can be tested in wind tunnels; (3) the large chord Reynolds number envelope (greater than 40 million); and (4) the ability to define small increments in friction drag between two test surfaces. Data are presented from experiments that demonstrate some of the capabilities of the FTF, including the shuttle thermal protection system airload tests, instrument development, and base drag studies. Proposed skin friction experiments and instrument evaluation studies are also discussed.

17. Key Words (Suggested by Author(s)) High Reynolds number Skin-friction drag Base drag Boundary layer measurements Pressure distributions	18. Distribution Statement Unclassified-Unlimited Star category 09

19. Security Classif. (of this report) Unclassified	20. Security Classif. (of this page) Unclassified	21. No. of Pages 17	22. Price* A02

*For sale by the National Technical Information Service, Springfield, Virginia 22161